Published in final edited form as:
J Med Chem. 2013 February 14; 56(3): 867–878. doi:10.1021/jm301338q.

Sulfated Pentagalloylglucoside is a Potent, Allosteric, and Selective Inhibitor of Factor XIa

Rami A. Al-Horani[1], **Pooja Ponnusamy**[1], **Akul Y. Mehta**[1], **David Gailani**[2], and **Umesh R. Desai**[*,1]

[1]Department of Medicinal Chemistry and Institute for Structural Biology and Drug Discovery, Virginia Commonwealth University, Richmond, VA 23219, USA

[2]Department of Pathology, Immunology and Microbiology, Vanderbilt University Medical Center, Nashville, TN 37203

Abstract

Inhibition of factor XIa (FXIa) is a novel paradigm for developing anticoagulants without major bleeding consequences. We present the discovery of sulfated pentagalloylglucoside (**6**) as a highly selective inhibitor of human FXIa. Biochemical screening of a focused library led to the identification of **6**, a sulfated aromatic mimetic of heparin. Inhibitor **6** displayed a potency of 551 nM against FXIa, which was at least 200-fold more selective than other relevant enzymes. It also prevented activation of factor IX and prolonged human plasma and whole blood clotting. Inhibitor **6** reduced V_{MAX} of FXIa hydrolysis of chromogenic substrate without affecting the K_M suggesting an allosteric mechanism. Competitive studies showed that **6** bound in the heparin-binding site of FXIa. No allosteric small molecule has been discovered to date that exhibits equivalent potency against FXIa. Inhibitor **6** is expected to open up a major route to allosteric FXIa anticoagulants with clinical relevance.

Keywords

Allosteric inhibition; Anticoagulants; Coagulation enzymes; Heparin mimetics

Introduction

Despite the advances made in recent years, thrombotic disorders such as venous thromboembolism and pulmonary embolism continue to thwart physicians and surgeons in imparting effective and safe anticoagulant therapy. Current anticoagulants used for treating these disorders include the heparins, coumarins, hirudins, and peptidomimetics.[1] The primary target of these agents are two key proteases, thrombin and factor Xa, which belong to the common pathway of the coagulation cascade. These agents enjoy considerable success owing to their high efficacy and relatively low cost to benefit ratio. However, heparins and coumarins suffer from many adverse effects, especially enhanced risk of bleeding.[2–4] The safety profile of newer oral peptidomimetic anticoagulants including dabigatran and rivaroxaban is being currently evaluated[5] and much remains to be known about their effects with cancer[6,7] and pregnancy.[8]

Address correspondence to: Umesh R. Desai, Department of Medicinal Chemistry, Virginia Commonwealth University, 800 E. Leigh Street, Suite 212, Richmond, VA 23219. Ph. 804-828-7328, Fax 804-827-3664, urdesai@vcu.edu.

Supporting Information

ESI-MS spectra, SIR, FXIa inhibition, *IC50's*, and UPLC-MS of three batches of **6** as well as APTT and PT studies of **2** and **4** are provided. This material is available free of charge via the internet at http://pubs.acs.org.

It is generally recognized that factor Xa and thrombin are important from both initiation and propagation perspectives, while proteases belonging to the intrinsic pathway are primarily involved in amplification of the coagulation signal.[1] A paradigm that is beginning to take shape is that targeting proteases of the intrinsic pathway, especially factor XIa (FXIa), may serve as a powerful route to antithrombotics that are safer than those that inhibit factor Xa and thrombin. A key foundation for this paradigm arises from recent studies indicating that depleting FXIa levels reduces thrombotic complications, while leaving the hemostatic process largely intact.[9–11] Absence of factor XI (FXI), the zymogen of FXIa, results in a rather mild bleeding disorder,[12–14] which is easily corrected by replacement with soluble, recombinant FXI. The occurrence of ischemic stroke[15] was also found to be significantly reduced in FXI-deficient patients. At the same time, elevated FXI levels enhanced risk for venous thrombosis[16] and cardiovascular disease in women.[17] These epidemiological studies are supported by genetic studies in mouse, which demonstrate that FXI-null mice do not develop clots in $FeCl_3$-induced carotid artery model, while showing no effect on bleeding time.[18]

Human FXIa is a plasma serine protease that is considerably different from other coagulation proteases. It is a disulfide-linked homodimer, in which each monomer consists of 607 amino acid residues that form four apple domains A1 through A4 and a trypsin-like catalytic domain.[19] The apple domains of FXI recognize factor IX (FIX), heparin/heparan sulfate, platelet glycoprotein GPIb, and other ligands to facilitate proteolytic function of FXIa and introduce a physiologic response. FXIa activation of FIX results in accelerated thrombin generation, which results in clot formation,[19,20] while GPIb binding probably contributes to localization of fibrin formation at the site of injury.[21,22]

A heparin-binding site (HBS) is present on the A3 domain of both the zymogen and the protease, and has been shown to contribute to serpin inhibition of FXIa through a template-mediated process.[23,24] Interestingly, FXIa also displays another HBS in its catalytic domain,[25] which binds the sulfated polysaccharide and other polyanions with approximately 100-fold higher affinity than the A3 site.[25,26] The HBS of the catalytic domain contributes less to templatemediated inhibition and more to allosteric or charge neutralization-based inhibition of FXIa by serpins.[27]

We reasoned that targeting the HBS of FXIa using small, designed molecule(s) may yield an effective inhibitor of this important intrinsic pathway enzyme that may be devoid of the major bleeding consequences noted with thrombin and factor Xa inhibitors. Such an inhibitor would function through an allosteric mechanism offering significant advantages in comparison to the traditional active site inhibitors. For example, an allosteric inhibitor is expected to be more selective than an orthosteric inhibitor because the active sites of coagulation enzymes are rather similar (each prefers a P-1 arginine) resulting in difficulties of selectivity. Allosteric sites, on the other hand, are much less conserved and structurally significantly different resulting in higher selectivity. This concept has been recently demonstrated with allosteric inhibitors of human α-thrombin.[28,29]

A survey of literature reveals that very few small molecule inhibitors of FXIa have been discovered so far. These include the arginine–containing acyclic peptidomimetics,[30,31] guanidine-containing aryl boronic acids[32] and β-lactam derivatives,[33,34] guanidine-containing natural products clavatadines A and B,[35] and amidine-containing macrocyclic indoles.[36] Each of these contain a strongly basic group that enforces recognition of the active site Asp189 resulting in competitive inhibition. Some of these inhibitors, in addition, also contain groups that covalently target the active site Ser195, e.g., boronic acids[32] and carbamates,[35] resulting in irreversible inhibition. Except for clavatadines, nearly every FXIa inhibitor discovered has been designed on the basis of a scaffold that recognizes thrombin.

Interestingly, recently two nonbasic, nonpeptidic inhibitors of α-thrombin were cocrystallized with FXIa, which may lead to new nonbasic FXIa-selective molecules.[37]

A key challenge in the design of these inhibitors has been achieving a combination of reasonable selectivity and potency against FXIa. Because coagulation enzymes are trypsin-like proteases, which prefer an arginine or an arginine-like P-1 group, selectivity has to rely on small differences in the binding pocket arising from the many loops surrounding the active site. In this respect, perhaps the only active site relatively easy to target is that of thrombin, which is constrained by the 60-loop.

In light of the observation that no allosteric inhibitors of FXIa have been reported so far and the promise of higher selectivity that an allosteric binding site presents, we screened a focused library of sulfated small molecule scaffolds belonging to the flavonoid, tetrahydroisoquinoline, cinammic acid, and gallic acid series (Figure 1). The non-saccharide library was developed in-house to mimic sulfated glycosaminoglycan (GAG) structures and contains several scaffolds chosen to yield good structural diversity. Only one molecule from this library, i.e., sulfated pentagalloylglucoside (**6**), was found to inhibit FXIa *in vitro* and *ex vivo*. Inhibitor **6** can be synthesized in few steps and is an aromatic GAG mimetic with several sulfate groups. Most importantly, **6** was found to selectively inhibit FXIa from among several coagulation enzymes and utilized the allosteric inhibition mechanism by interacting with the HBS of the catalytic domain of FXIa, as expected on the basis of the GAG-mimicking nature. Molecule **6** is the first inhibitor that displays such interesting properties and we expect it should catalyze a major route to the design and discovery of a new series of allosteric anticoagulants.

Experimental Procedures

Chemicals, Reagents, and Proteins

Anhydrous CH_2Cl_2, THF, CH_3CN, DMF, methanol, acetone and HPLC grade solvents (acetonitrile and formic acid) were purchased from Sigma-Aldrich (Milwaukee, WI) or Fisher (Pittsburgh, PA) and used as such. Chemical reactions sensitive to air or moisture were carried out under nitrogen atmosphere in oven-dried glassware. Reagent solutions, unless otherwise noted, were handled under a nitrogen atmosphere using syringe techniques. n-Hexylamine for ion-pairing UPLC was from Acros Organics (Morris Plains, NJ).

Human plasma proteases including thrombin, factor Xa, FXIa, factor IXa, factor VIIa, and recombinant tissue factor were obtained from Haematologic Technologies (Essex Junction, VT). Recombinant human FXIa and the isolated FXIa catalytic domain (FXIa-CD), used in the Gailani laboratory, were prepared as described earlier.[27,38] Factor XIIa was purchased from Enzyme Research Laboratories (South Bend, IN). Bovine α-chymotrypsin and bovine trypsin were obtained from Sigma-Aldrich (St. Louis, MO). Stock solutions of factor XIa, thrombin, factor XIIa, trypsin, and chymotrypsin were prepared in 50 mM TrisHCl buffer, pH 7.4, containing 150 mM NaCl, 0.1% PEG8000, and 0.02% Tween80. Stock solutions of factor Xa and factor VIIa were prepared in 20 mM TrisHCl buffer, pH 7.4, containing 100 mM NaCl, 2.5 mM $CaCl_2$, 0.1% PEG8000, and 0.02% Tween80. Stock solution of factor IXa was prepared in 20 mM TrisHCl buffer, pH 7.4, containing 100 mM NaCl, 2.5 mM $CaCl_2$, 0.1% PEG8000, 0.02% Tween80, and 33% v/v ethyleneglycol.

Chromogenic substrates, Spectrozyme TH (H-*D*-hexahydrotyrosol-Ala-Arg-*p*-nitroanilide), Spectrozyme factor Xa (Methoxycarbonyl-*D*-cyclohexylglycyl-Gly-Arg-*p*-nitroanilide), Spectrozyme FXIIa (*D*-ctclohydrotyrosyl-glycyl-*L*-Arg-*p*-nitroanilide diacetate salt), Spectrozyme FIXa (*D*-leucyl-phenylglycyl-Arg-*p*-nitroanilide diacetate), Spectrozyme factor VIIa (Methanesulphonyl-*D*-cyclohexylalanyl-butyl-Arg-*p*-nitroanilide), and

Spectrozyme CTY were obtained from American Diagnostica (Greenwich, CT). Factor XIa chromogenic substrate (S-2366, H-*D*-Val-Leu-Arg-*p*-nitroanilide.2HCl) and trypsin substrate (S-2222, Benzyl-Ile-Glu(γ–OH and −OCH_3)-Gly-Arg-*p*-nitroanilide·HCl) were obtained from Diapharma (West Chester, OH). Bovine unfractionated heparin (UFH) was purchased from Sigma-Aldrich (St. Louis, MO). Pooled normal human plasma for coagulation assays was purchased from Valley Biomedical (Winchester, VA). Activated partial thromboplastin time reagent containing ellagic acid (APTT-LS), thromboplastin-D, and 25 mM $CaCl_2$ were obtained from Fisher Diagnostics (Middletown, VA). Thromboelastograph® Coagulation Analyzer 5000 (TEG®), disposable cups and pins, and 200 mM stock $CaCl_2$ were obtained from Haemoscope Corporation (Niles, IL).

Purification of Chemically Synthesized Molecules

Analytical TLC was performed using UNIPLATE™ silica gel GHLF 250 um pre-coated plates (ANALTECH, Newark, DE). Column chromatography was performed using silica gel (200–400 mesh, 60 Å) from Sigma-Aldrich. Flash chromatography was performed using Teledyne ISCO (Lincoln, NE) Combiflash RF system and disposable normal silica cartridges of 30–50 μ particle size, 230–400 mesh size and 60 Å pore size. The flow rate of the mobile phase was in the range of 18 to 35 mL/min and mobile phase gradients of ethyl acetate/hexanes and CH_2Cl_2/CH_3OH were used to elute unsulfated compounds.

Sulfated molecules were purified using Sephadex G10 size exclusion chromatography. The quaternary ammonium counter ion of sulfate groups present in the molecules was exchanged for sodium ion using SP Sephadex-Na cation exchange chromatography. Sephadex G10 and SP Sephadex-Na chromatographies were performed using Flex columns (KIMBLE/KONTES, Vineland, NJ) of dimensions 170 × 1.5 cm and 75 × 1.5 cm, respectively. For regeneration of the cation exchange column, 1 L of 2 M NaCl solution was used. Water was used as eluent in both chromatographies. Five mL fractions were collected and analyzed by capillary electrophoresis (CE). CE experiments were performed using a Beckman P/ACE MDQ system (Fullerton, CA). Electrophoresis was performed at 25 °C and a constant voltage of 8 kV or a constant current of 75 μA using an uncoated fused silica capillary (ID 75 μm) with the total and effective lengths of 31.2 cm and 21 cm, respectively. A sequential wash of 1M HCl (10 min), water (3 min), 1M NaOH (10 min), and water (3 min) at 20 psi was used to activate the capillary. Before each run, the capillary was rinsed with the run buffer; 50 mM sodium phosphate buffer of pH=3, for 3 min at 20 psi. Sulfated compounds injected at the cathode (0.5 psi for 4 s) and detected at the anode (214 nm). The purity of each sulfated compound, as determined by CE, was greater than 95%.

Chemical Synthesis of Diversified Library of Sulfated Molecules

The polyphenolic precursors of the sulfated molecules were either commercially available as silibinin (**1**), chlorogenic acid (**3**), and pentagalloyl glucopyranoside (**5**) or were chemically synthesized as reported earlier for polyphenolic 1,2,3,4-tetrahydroisoquinoline (THIQ) derivatives (**7–14**) (see Figure 1).[40,41] Briefly, synthesis of polyphenolic THIQ derivatives was achieved in quantitative yields using Horner–Wadsworth–Emmons and Pictet–Spengler reactions followed by EDCI– mediated amidation and BBr_3–assisted deprotection.[40] Sulfated silibinin (**2**) and sulfated chlorogenic acid (**4**) were synthesized by the microwave–assisted synthesis developed earlier.[41] Briefly, the polyphenolic precursors (**1**, **3**, and **5**) and trimethylamine–sulfur trioxide (5 equivalents/–OH group) were mixed in equivolume mixture of DMF and CH_3CN (3 mL) in microwave tube. The reaction tube was sealed and microwaved (CEM-discover microwave synthesizer) for 0.5–2 h at 100 °C. Sulfated THIQ derivatives were synthesized in an equivolume mixture of DMF and CH_3CN (3 mL) containing the trimethylamine–sulfur trioxide complex (6 equivalents/−OH group) which was heated for 5 h at 80 °C.

Synthesis of sulfated pentagalloyl glucoside (6)

Pentagalloyl glucopyranoside (**5**) (25 mg, 0.027 mmol) was sulfated in DMF:CH_3CN mixture (3 mL) using trimethylamine–sulfur trioxide complex (281 mg, 2.03 mmol). The reaction mixture was microwaved at 100 °C for 2 h. The resulting crude product was cooled and concentrated in vacuum at temperature less than 35 °C. It was purified as described above using the size exclusion chromatography (G-10). The sodium salt form of **6**, the isolated white fluffy solid mixture (42 mg, 63%), was generated by the sodium exchange chromatography as described above. The synthesis was respeated three times under similar conditions.

Characterization of Synthetic Compounds

Each compound was characterized using ^1H and ^{13}C NMR spectroscopy, which was performed on Bruker 400 MHz spectrometer in either $CDCl_3$, CD_3OD, acetone-d_6, or D_2O. Signals, in part per million (ppm), are either relative to the internal standard (tetramethyl silane, TMS) or to the residual peak of the solvent. The NMR data are reported as chemical shift (ppm), multiplicity of signal (s= singlet, d= doublet, t= triplet, q= quartet, dd= doublet of doublet, m= multiplet), coupling constants (Hz), and integration. ESI MS of unsulfated molecules were recorded using Waters Acquity TQD MS spectrometer in positive ion mode whereas ESI MS negative mode was used for sulfated compounds. Samples were dissolved in methanol or water and infused at a rate of 20 μL/min. Mass scans were obtained, as reported earlier, for both unsulfated as well as sulfated compounds.[39,40] The NMR and MS data of polyphenolic and sulfated THIQ molecules were consistent with the reported values. We present here the data for newly synthesized molecules **2**, **4**, and **6**.

Sulfated Silibinin (2)

^1H-NMR (D_2O, 400 MHz): 7.44–7.41 (m, 1 H), 7.21–7.14 (m, 1 H), 7.10–7.0 (m, 4 H), 6.51–6.48 (m, 1 H), 6.44–6.42 (M, 1H), 5.33 (d, J = 10.2 Hz, 1H), 5.07– 5.02 (m, 1 H), 4.45–4.36 (m, 1 H), 4.22–4.17 (m, 1 H), 3.92–3.82 (m, 5 H). ^{13}C-NMR (D_2O, 100 MHz): 193.87, 161.92, 159.64, 151.63, 143.47, 142.96, 140.68, 134.08, 128.73, 123.16, 122.0, 121.81 117.23, 117.0, 112.8, 104.71, 101.85, 100.71, 81.3, 79.68, 76.0, 75.84, 66.68, 56.26. MS (ESI) calculated for $C_{25}H_{18}Na_4O_{22}S_4$, $[M–Na]^—$, *m/z* 867.60, found for $[M–Na]^—$, *m/z* 867.80.

Sulfated Chlorogenic Acid (4)

^1H-NMR (D_2O, 400 MHz): 7.80 (d, J = 12.5 Hz, 1 H), 7.74 (s, 1 H), 7.62–7.60 (m, 2 H), 6.58 (d, J =16.0 Hz, 1 H), 5.69–5.64 (m, 1 H), 5.19–5.15 (m, 1 H), 4.80–4.75 (m, 1 H), 2.63–2.51 (m, 4 H). ^{13}C-NMR (D_2O, 100 MHz): 175.74, 167.41, 144.88, 143.27, 132.86, 127.24, 123.32, 122.98, 118.20, 83.50, 75.52, 73.98, 68.31, 34.85, 33.91. MS (ESI) calculated for $C_{16}H_{13}Na_5O_{21}S_4$, $[M–Na]^—$, *m/z* 760.84, found for $[M–Na]^—$, *m/z* 760.48.

Sulfated Pentagalloylglucoside (6)

^1H-NMR (D_2O, 400 MHz): 8.11–7.40 (m, 10 H), 6.51–6.47 (m, 1 H), 6.11–6.18 (m, 1 H), 5.79–5.97 (m, 2 H), 4.85–4.60 (m, 3 H). ^{13}C-NMR (D_2O, 100 MHz): 166.39, 165.70, 165.40, 164.71, 150.62, 150.53, 147.82, 147.43, 147.17, 145.69, 145.53, 126.34, 122.42, 122.22, 122.17, 121.98, 120.97, 119.74, 118.99, 118.69, 115.32, 93.04, 74.5, 72.24, 71.59, 68.90, 63.50.

UPLC-MS Characterization of 6

Waters Acquity H-class UPLC system equipped with a photodiode array detector and triple quadrupole mass spectrometer was used for characterization of **6**. A reversed-phase Waters

BEH C18 column of particle size 1.7 μ and 2.1×50 mm dimensions at 30±2°C was used for separation of its components. Solvent A consisted of 25 mM n-hexylamine in water containing 0.1% (v/v) formic acid, while solvent B consisted of 25 mM *n*-hexylamine in acetonitrile–water mixture (3:1 v/v) containing 0.1% (v/v) formic acid. Resolution of **6** into distinct peaks was achieved with a flow rate of 500 μL/min and a linear gradient of 3% solvent B per min over 20 min (initial solvent B proportion was 20% v/v). The sample was first monitored for absorbance in the range of 190–400 nm and then directly introduced into the mass spectrometer. ESI-MS detection was performed in positive ion mode for which the capillary voltage was 4 kV, cone voltage was 20 V, desolvation temperature was 350°C and nitrogen gas flow was maintained at 650 L/hr. Mass scans were collected in the range of 1000–2048 amu within 0.25 s and several of these added to enhanced signal-to-noise ratio.

Direct Inhibition of Factor XIa

Direct inhibition of FXIa was measured by a chromogenic substrate hydrolysis assay, as reported earlier[42] using a microplate reader (FlexStation III, Molecular Devices) at 37 °C. Generally, each well of the 96-well microplate contained 85 μL pH 7.4 buffer to which 5 μL potential FXIa inhibitor (or solvent reference) and 5 μL FXIa (0.765 nM final concentration) were sequentially added. After 10 min incubation, 5 μL factor XIa substrate (345 μM) was rapidly added and the residual FXIa activity was measured from the initial rate of increase in absorbance at 405 nm. Stocks of potential FXIa inhibitors serially diluted to give twelve different aliquots in the wells. Relative residual FXIa activity at each concentration of the inhibitor was calculated from the ratio of FXIa activity in the presence and absence of the inhibitor. Logistic equation 1 was used to fit the dose–dependence of residual protease activity to obtain the potency (IC_{50}) and efficacy (ΔY) of inhibition. In this equation, Y is the ratio of residual factor XIa activity in the presence of inhibitor to that in its absence (fractional residual activity), Y_M and Y_0 are the maximum and minimum possible values of the fractional residual proteinase activity, IC_{50} is the concentration of the inhibitor that results in 50% inhibition of enzyme activity, and HS is the Hill slope. Nonlinear curve fitting resulted in Y_M, Y_0, IC_{50} and HS values.

$$Y = Y_0 + \frac{Y_M - Y_0}{1 + 10^{(log[I]_0 - log\ IC_{50})(HS)}} \quad \text{Eq. 1}$$

Inhibition of FXIa Activation of FIX by 6

Plasma FIX (500 nM) was incubated with human FXIa (3 nM) in 50 mM Hepes buffer, pH 7.4, containing 125 mM NaCl, 5 mM $CaCl_2$, and 0.1 mg/mL bovine serum albumin at 24 °C. At various incubation times, 7 μL aliquots were removed, mixed with 7 μL of reducing sample buffer (233 mM Tris-HCl, 138 mM SDS, 19% glycerol, 10% 2-mercaptoethanol, 0.01% bromophenol blue, pH 6.8), fractionated on 12% polyacrylamide-SDS gels, and then transferred to nitrocellulose. The primary antibody was goat anti-human FIX polyclonal IgG (Enzyme Research Laboratories, South Bend, IN), and the secondary antibody was horseradish peroxidase-conjugated anti-goat IgG. Detection was by chemiluminescence. The relative positions of FIX and FIXaβ bands were confirmed using Western blots of known standards for each protein.

Inhibition of Proteases of the Coagulation and Digestive Systems by 6

The inhibition potential of **6** against coagulation enzymes including thrombin, factor VIIa, factor IXa, factor Xa, and factor XIIa, and digestive enzymes including trypsin and chymotrypsin was evaluated using chromogenic substrate hydrolysis assays reported in the literature.[42] These assays were performed using substrates and conditions appropriate for the enzyme being studied. For selectivity analysis, at least six serially diluted concentrations of

6 were utilized and the fractional residual enzyme activity was measured at each concentration. The inhibition profile was determined over a range of inhibitor concentrations to determine the IC_{50} of the enzyme– inhibitor complex. The K_M of the substrate for its enzyme was used to identify the concentration of the substrate to be used for inhibition studies. The concentrations of enzymes and substrates in microplate cells were: 6 nM and 50 μM for thrombin; 1.09 nM and 125 μM for factor Xa; 5 nM and 125 μM for factor XIIa; 89 nM and 850 μM for factor IXa; 8 nM and 1000 μM for factor VIIa (along with 40 nM recombinant tissue factor); 72.5 ng/mL and 80 μM for bovine trypsin; and 500 ng/mL and 240 μM for bovine chymotrypsin.

Michaelis–Menten Kinetics of Substrate Hydrolysis by Factor XIa in Presence of 6

The initial rate of S-2366 hydrolysis by either wild-type FXIa (3 nM) or FXIa catalytic domain (6 nM) was obtained from the linear increase in absorbance at 405 nM corresponding to less than 10% consumption of the chromogenic substrate. The initial rate was measured as a function of various concentrations of the substrate (0–2 mM) in the presence of fixed concentration of **6** (0–50 μg/mL) in 50 mM Tris-HCl buffer, pH 7.6, containing 150 mM NaCl, 0.1 mg/mL bovine serum albumin and 5 mM $CaCl_2$. Active site concentrations for preparations of FXIa were determined by titrations with human antithrombin in an S-2366 cleavage assay. The reaction was monitored using a SpectraMax 340 microtiter plate reader (Molecular Devices Corp., Sunnyvale, CA) with a reaction volume of 100 μL and path length of 3 mm. Each assay was performed in triplicate. The concentration of S-2366 was measured using an absorption coefficient of 8,266 $M^{-1}cm^{-1}$ at λ_{342} nm, while the free *p*-nitroaniline concentration was calculated using an absorption coefficient of 9,933 $M^{-1}cm^{-1}$ at λ_{405} nm. The data was fitted using the standard Michaelis–Menten Eq. 2 to determine the K_M and V_{MAX}.

$$V = \frac{V_{MAX}[S]}{K_M + [S]} \quad \text{Eq. 2}$$

Determination of the Equilibrium Dissociation Constant of UFH to Factor XIa

The equilibrium binding constant (K_D) of UFH to FXIa was determined by fluorescence spectroscopy. Fluorescence experiments were performed using a QM4 fluorometer (Photon Technology International, Birmingham, NJ) in 20 mM sodium phosphate buffer of pH 7.4 containing 100 mM NaCl, 0.1 mM EDTA, and 0.1% PEG8000 at 37 °C. The K_D for the interaction of UFH with human FXIa was determined by titrating the UFH (200 μM) into a solution of FXIa (25 nM) and monitoring the decrease in the intrinsic fluorescence of FXIa at 340 nm (λ_{ex} = 280 nm). The slit widths on the excitation and emission side were 1 mm in both cases. The decrease in fluorescence signal was fitted using the quadratic equilibrium binding equation 3 to obtain the K_D of interaction. In this equation, ΔF represents the change in fluorescence following each addition of UFH from the initial fluorescence F_o and ΔF_{MAX} represents the maximal change in fluorescence observed on saturation of FXIa.

$$\frac{\Delta F}{F_0} = \frac{\Delta F_{MAX}}{F_0} \times \frac{([FXIa]_0 + [UFH]_0 + K_D) - \sqrt{([FXIa]_0 + [UFH]_0 + K_D)^2 - 4[FXIa]_0[UFH]_0}}{2[FXIa]_0} \quad \text{Eq. 3}$$

Competitive Binding Studies of 6 with UFH

Inhibition of FXIa by **6** was performed in the presence of UFH using the 96–well plate format. A 5 μL solution of **6** (0–27.5 μg/mL in the well) and 5 μL of factor XIa (0.765 nM in the well) with 5μL of UFH (0–33.3 μM in the well) in 80 μL of 50 mM TrisHCl buffer, pH

7.4, containing 150 mM NaCl, 0.1% PEG8000, and 0.02% Tween80 was incubated at 37 °C for 10 min. Following incubation, 5 μL of FXIa substrate (345 μM in the well) was added and the initial change in absorbance at 405 nm measured. The dose dependence of the fractional residual proteinase activity at each concentration of the competitor was fitted by Eq. 1 to obtain the apparent concentration of **6** required to reduce FXIa activity to 50% of its initial value ($IC_{50,predicted}$). Quantitative comparison of competitive binding was performed using the Dixon−Webb relationship (Eq. 4). In this equation, $K_{D,UFH}$ is the dissociation constant of FXIa−UFH complex, which was measured above.

$$IC_{50,predicted} = IC_{50}\left(1+\frac{[UFH]_0}{K_{D,UFH}}\right) \quad \text{Eq. 4}$$

Prothrombin Time (PT) and Activated Partial ThromboplastinTime (APTT)

Clotting time was measured in a standard one–stage recalcification assay with a BBL Fibrosystem fibrometer (Becton-Dickinson, Sparles, MD), as described previously.[43–46] For PT assays, thromboplastin-D was reconstituted according to the manufacturer's directions and warmed to 37 °C. A 10 μL solution of **6**, to give the desired concentration, was brought up to 100 μL with citrated human plasma, incubated for 30 s at 37° C followed by addition of 200 μL of prewarmed thromboplastin-D. For the APTT assay, 10 μL of **6** was mixed with 90 μL of citrated human plasma and 100 μL of prewarmed APTT reagent (0.2% ellagic acid). After incubation for 4 min at 37 °C, clotting was initiated by adding 100 μL of prewarmed 25 mM $CaCl_2$ and time to clot noted. The data were fit to a quadratic trend line, which was used to determine the concentration of the inhibitor necessary to double the clotting time. Clotting time in the absence of an anticoagulant was determined in similar fashion using 10 μL of deionized water and/or appropriate organic vehicle and was found to be 18.9 s for PT and 42.4 s for APTT.

Thromboelastography (TEG®) Analysis of Clot Formation in Presence of 6

TEG® assays were performed essentially as reported earlier.[43–46] Briefly, the assays were initiated by transferring 20 μL of 200 mM $CaCl_2$ into the Haemoscope™ disposable cup, oscillating through 4° 45′ angle at 0.1 Hz, followed by the addition of a mixture of 340 μL of sodium citrated whole blood containing 10 μL of **6** or high pure water at 37 °C. This recalcification initiates clot formation in the TEG® coagulation analyzer, which operates until all necessary data collection including R (reaction time in min.), α (angle in degs.), MA (maximum amplitude, mm), and G (shear elastic modulus in kDynes/cm_3) is completed in an automated manner.

Results

Library of Polyphenolic and Sulfated Molecules

At the outset, the fundamental idea in discovering allosteric FXIa inhibitors was to screen GAG mimetics that potentially bind the HBS and induce an inhibitory conformational change in the active site. Our laboratory has previously developed a large number of small, non-saccharide GAG mimetics including sulfated flavonoids,[47] sulfated benzofurans,[28] and sulfated THIQ derivatives.[39] Considering the size of the HBS on FXIa, we studied silibinin (**1**) and its sulfated derivative (**2**), chlorogenic acid (**3**) and its sulfated derivative (**4**), pentagalloylglucoside (**5**) and its sulfated derivative (**6**), and the library of THIQ derivatives (**7–14**), which was synthesized earlier.[39] These structures contain significantly diverse structures, especially in terms of placement of multiple sulfate groups, that could be expected to mimic heparin's interaction with FXIa.

Sulfated silibinin (**2**), sulfated chlorogenic acid (**4**), and sulfated pentagalloylglucoside (**6**) were synthesized by the microwave–assisted sulfation strategy,[41] while sulfated THIQ derivatives were synthesized by sulfation by heating the reaction mixture for 5 hrs at 80 °C.[47] In either case, sulfation was high yielding (>60%). Each sulfated molecule was homogeneous, i.e., containing a single sulfated species, as assessed by capillary electrophoresis and detailed ^{1}H NMR, ^{13}C NMR and ESI-MS techniques, except for **6**, which showed partially sulfated species as described below.

Structure Determination of 6

The capillary electrophoretic profile of **6** in reverse polarity mode displayed a complex, ill-resolved pattern indicating the presence of partially sulfated components (not shown). To identify the proportion and structure of these components, we resorted to reversed-phase ion-pairing UPLC, a technique that has found good utility in resolving highly sulfated GAGs and related molecules.[48] In this technique, an ion-pairing agent, such as *n*-hexylamine, is introduced in the mobile phase so as to replace sodium cations present on each sulfate group and impart considerable hydrophobicity to the molecule. Resolution arises from the different hydrophobicities of the constituents that contain varying number of nhexylamine groups. The UPLC profile of **6** showed the presence of six major nearly baseline resolved peaks, labeled *p1* through *p6* in Figure 2, each of which was found to further containing multiple peaks.

The ESI-MS profile of each peak, observed between 1000 and 2048 m/z range, was found to contain a doubly charged molecular ion with a general formula of $[(PGG+n\times SO_3\text{-}HXA-n\times H)+2\times HXA]^{2+}$, where *n* is the number of sulfonate (SO_3^-)-hexylammonium (HXA) ionpairs present in the molecule (see Figures S1 through S5 of Supporting Information). For example, peaks *p3*, *p4* and *p5* displayed molecular ions at 1388.43, 1478.99 and 1569.60 *m/z*, respectively, corresponding to doubly charged **6** species containing 9, 10 and 11 sulfate groups with 11, 12 and 13 *n*-hexylamines, respectively, as ion-pairs. A similar behavior was observed for peaks *p1, p2* and *p6*, which corresponded to **6** species with 7, 8 and 12 sulfate groups, respectively. In addition to the molecular ions, the MS also displayed several other ions corresponding to the loss of one or more hexylamine-paired sulfonate groups further confirming the identity of the parent sulfated species.

To identify the origin of multiple components observed within peaks *p1* through *p6*, we utilized selective ion recording (SIR)-MS. In this technique, the spectrometer is tuned to monitor a specific ion, e.g., 1478.99 *m/z* corresponding to $[M+10\ SO_3+12\ \text{hexylamines}]^{2+}$ ion, resulting in the identification of all peaks that contain this molecular ion. Figure 2 shows three SIR profiles of **6**. Monitoring at 1388.43 *m/z* gave a SIR profile that essentially mimicked *p3* of the UV chromatogram suggesting that each component present in the *p3* peak contained nine sulfate groups. More importantly, the ion corresponding to 1388.43 was not present in any peak other than *p3*. Likewise, monitoring at 1478.99 or 1569.90 *m/z* resulted in a profile equivalent to chromatographic peaks *p4* or *p5*, respectively. This was also found to be the case for peaks *p1*, *p2* and *p6* (see Figure S6). To further confirm the consistency of this assignment, the synthesis of **6** was repeated twice. An essentially similar composition of major peaks was obtained as identified by UPLC-MS and SIR analysis (see Figure S7).

In combination, UPLC-MS coupled with SIR analysis suggested that **6** is a mixture of septa- (*p1*), octa- (*p2*), nona- (*p3*), deca- (*p4*), undeca- (*p5*) and dodeca- (*p6*) sulfated species, which further contain sub-species with an identical number of sulfate groups. We predict that the sub-species arise due to variably positioned sulfate groups within each family of peaks. This enhances the structural diversity of **6**. Analysis of the UPLC profile gave a composition of 6%, 17%, 21%, 45%, 11% and 3% *p1* through *p6*, respectively (Figure 2).

Using these and their associated molecular weights, the weight-average molecular weight of **6** was calculated to be 2178 (Na^+ form).

Factor XIa Inhibition Potential of Synthetic, Sulfated Heparin Mimetics

Each sulfated molecule of the library was evaluated for its potential to inhibit FXIa hydrolysis of S-2366, a chromogenic small peptide substrate, at pH 7.4 and 37°C as reported earlier.[43] Whereas the presence of **6** resulted in a dose-dependent reduction in FXIa activity, none of the other sulfated derivatives **2**, **4** or **7** – **14** demonstrated any effect at concentrations as high as 250 μM. The dose-dependence of FXIa activity could be fitted using the logistic equation 1, which resulted in an IC_{50} of 1.2 ± 0.1 μg/mL with an efficacy of 97% and Hill slope of 1.3 (Figure 3, Table 1). The IC_{50} values for **6**, prepared in two independent synthetic efforts, was essentially identical (see Figure S8 and Table S1). Taking into consideration the average molecular weight of **6** deduced above, i.e., 2178 g/mol, the IC_{50} translates to 551 ± 32 nM, which makes it the most active FXIa inhibitor reported in literature to date. The lack of inhibition potential for the **2**, **4** and sulfated THIQ derivatives suggests a rather selective interaction between FXIa and **6**, although more work will be necessary to extract key structural requirements in **6** that induce inhibition.

To assess the importance of sulfate groups in **6**, its polyphenolic precursor **5** was evaluated for inhibition of FXIa proteolytic activity. Molecule **5** was found to be completely inactive at the highest concentration tested (300 μM) highlighting the significance of sulfate groups. The result supports the idea that **6**'s heparin mimicking action is likely to be the basis for its interaction with FXIa.

Inhibition of FXIa Activation of Physiologically Relevant Substrate FIX by 6

Although **6** inhibits FXIa hydrolysis of chromogenic substrate S-2366, FIX is the more relevant substrate of FXIa. During coagulation, FXIa activates FIX through cleavages at two sites (Arg145-Ala146 and Arg180-Val181) in rapid succession so as to generate FIXaβ,[49] which helps form the intrinsic tenase complex eventually accelerating thrombin production. FIX binds to the A3 domain of FXIa followed by cleavages at these two sites.[50] Such exosite-mediated associations can bring about widespread conformational changes in either proteins raising concern about the translation of **6** inhibition of tripeptidyl substrate hydrolysis to physiological macromolecules. Hence, we measured FXIa activation of FIX in the presence and absence of **6** using Western blotting. Figure 4 shows the time profile of FXIa incubated with a high concentration of FIX (0.5 μM) under pseudo-first order conditions with **6** at 3 μM. The profile reveals that even after 120 min of incubation, formation of FIXaβ was not detectable, while control experiments show nearly quantitative activation of FIX within less than 30 min. Although densitometric analysis was not attempted, the study shows nearly 100% efficacy of inhibition of FIX activation by FXIa in the presence of **6**, which is similar to that observed in hydrolysis of chromogenic substrate.

Selective Inhibition of FXIa over Other Coagulation and Digestive Proteases by 6

The inhibition profiles of **6** against the coagulation factors IIa, VIIa, IXa, Xa, and XIIa as well as against related serine proteases of digestive system, such as trypsin and chymotrypsin, were studied using the substrate hydrolysis assays, as described earlier.[43] In these assays, the inhibition potential was determined by spectrophotometric measurement of the residual protease activity in the presence of varying concentrations of **6**. Figure 3 displays the decrease in the protease activity over the range of 0.01—10,000 μg/mL, which was fitted using equation 1 to calculate the IC_{50} (Table 1). Molecule **6** inhibits human factors IIa, IXa, Xa, and XIIa, although the potency (265–1219 μg/mL) is much weaker than that for FXIa. Particularly, **6** demonstrated selectivity of 200–fold over factor XIIa, 221–fold

over factor Xa, 950–fold over factor IXa, and 1016–fold over thrombin. In contrast, no inhibition was observed up to concentrations as high as 1.8 mg/mL for trypsin and chymotrypsin, and 3.7 mg/mL for factor VIIa. These results suggested that **6** is a selective inhibitor for human FXIa.

Allosteric Inhibition of Factor XIa by 6

To understand the mechanistic basis of inhibition, Michaelis–Menten kinetics of S-2366 hydrolysis by recombinant wild type, full-length FXIa was performed in the presence of **6** at pH 7.4 and 37 °C. In addition, a FXIa species containing only the catalytic domain, i.e., FXIa-CD, was also studied. Figure 5 shows the initial rate profiles in the presence of **6** (0–50 μg/mL). Each profile displays a characteristic rectangular hyperbolic dependence, which could be fitted using equation 2 to give the apparent K_M and V_{MAX} Table 2). With wild-type FXIa, the K_M for S-2366 remained essentially unchanged in the presence or absence of **6** at ~0.5 μM, while the V_{MAX} decreased steadily from 120.9 mAU/min in the absence of **6** to 17.2 mAU/min at 50 μg/mL of **6**. Likewise, the FXIa-CD displayed an essentially similar profile. The K_M for S-2366 hydrolysis in the absence of **6** was found to be 0.53 μM, which remained invariant in the presence of **6** (0.005 to 5.0 μg/mL). In contrast, V_{MAX} decreased nearly 5-fold from 117.3 mAU/min to 22.6 mAU/min (Figure 5, Table 2). Thus, **6** brings about structural changes in the active site of FXIa, which does not affect the formation of Michaelis complex, but induces a significant dysfunction in the catalytic apparatus. This indicates that **6** is an allosteric inhibitor of human FXIa. Further, the study also shows that **6** binds to the catalytic domain to induce allosteric dysfunction.

Inhibitor 6 Binds in the Heparin Binding Site of Factor XIa

To assess whether **6** is a heparin mimetic, we measured inhibition of FXIa in presence of unfractionated heparin (UFH). As discussed in the introduction, FXIa possesses two binding sites for UFH – one on the A3 domain and the other in the catalytic domain. To study competition between **6** and UFH, we first measured the affinity of UFH to FXIa through the change in the intrinsic fluorescence of FXIa. UFH induces a saturable decrease of tryptophan fluorescence by ~15% which gave the K_D of UFH–FXIa complex (1.5 ± 0.2 μM).

Figure 6A shows the change in dose–response profiles of **6** inhibiting FXIa in the presence of UFH at pH 7.4 and 37 °C. As the concentration of UFH increased from 0.13 μM to 33.3 μM, the IC_{50} of FXIa inhibition increased from 1.2 μg/mL to 31.4 μg/mL (Table 3). A more quantitative test of competitive binding is the Dixon–Webb relationship (Eq. 4), which predicts the effect of an ideal competitor on a measured parameter, *e.g.* K_D or IC_{50}. Using this equation the $IC_{50,predicted}$ for **6** inhibition of FXIa at each UFH was calculated (Table 3). Figure 6B shows a comparison of the measured and predicted IC_{50}'s. Thus, **6**'s inhibition of FXIa stems from binding to or in the vicinity of heparin binding site on the enzyme's catalytic domain. This implies that **6** is an allosteric inhibitor and a small molecule heparin mimetic.

Inhibitor 6 is an Effective Anticoagulant in Human Plasma

Plasma clotting assays, prothrombin and activated partial thromboplastin time (PT and APTT, respectively), are routinely used to assess the anticoagulation potential of new enzyme inhibitors in an *in vitro* setting. Whereas PT measures the effect of an inhibitor on the extrinsic pathway of coagulation, APTT measures the effect on the intrinsic pathway. The concentrations of **6** required to double PT and APTT were measured, as described earlier.[43–46] Figure 7 shows the variation in PT and APTT in the presence of varying concentrations of **6**. A 2-fold increase in PT required 298 μg/mL of **6**. Likewise, a 2-fold

increase in the APTT required 96 μg/mL of **6**, only 18–fold less than that of enoxaparin, which displayed doubling of clottin time at 5.4 μg/mL in a similar assay.[43] In comparison, the APTT and PT values for molecules **2** and **4** were much higher (see Table S2). At molar levels, **6** turns out to be 36-fold less effective than enoxaparin. These results indicate that chemically synthesized **6** has good anticoagulation properties in human plasma.

Inhibitor 6 is an Effective Anticoagulant in Human Whole Blood as Indicated by Thromboelastography

To assess the anticoagulation properties of **6** in human whole blood, thromboelastography was employed. This technique is an *ex vivo* protocol often utilized to evaluate the anticoagulant activity of low molecular weight heparins (LMWHs) in whole blood.[43–46, 51,52] Thromboelastography monitors the thrombodynamic properties of blood as it is induced to clot under a low shear environment resembling sluggish venous flow. These thrombodynamic properties are expected to dramatically change in presence of anticoagulant in blood. The blood clot formation is recorded as a force transduced on a pin at the center of a blood–containing cup. The kinetics of clot formation and growth as well as the strength and stability of the formed clot are measured through parameters such as maximum amplitude (MA) of clot formation; shear elastic modulus strength (G) of clot; the reaction time (R) for the start of clotting; and the angle α, which is a measure of fibrin build-up and cross-linking (Figure 8).

Table 4 shows the effects of **6** and enoxaparin in human whole blood with respect to the changes in R, α, MA, and G parameters. For both anticoagulants, increasing the concentration increases R and decreases α, MA, and G parameters. Briefly, R increases from 6.0 min to 87.1 min as the concentration of **6** increases from 0 μg/mL to 280 μg/mL, while α decreases from 56.4° to less than 9.4° suggesting a significant decrease in the fibrin polymerization and network formation. Enoxaparin demonstrates similar effect on R and α parameters, except it exhibits such effects at a range of 0 to 4.5 μg/mL.[43] Over the same range, enoxaparin decreases MA and G measurements by about 1.5– and 2–fold, respectively. In similar fashion, **6** reduces MA and G by ~4– to 8–fold over the concentration range of 0–280 μg/mL. These results suggest that **6** is a good anticoagulant in human whole blood.

Discussion

To discover highly selective allosteric FXIa inhibitor, we focused on the heparin–FXIa interaction, which appears to play a major role in its physiologic function.[19,20,26,53] Screening a focused library of GAG mimetics resulted in the discovery of **6**, which possesses a core β-*D*-glucose unit decorated with five units of gallic acid. Chemical sulfation of PGG led to a mixture of septa, octa, nona, deca, undeca and dodeca -sulfated species (Figure 2), which translated into an average molecular weight of 2178 (Na^+ form). The major constituent was the deca-sulfated species, which corresponds to an average of two sulfate groups per aromatic ring. Our previous work has shown that the 3,4,5-trihydroxy phenyl ring is preferentially sulfated at the 3- and 5-positions because of steric inaccessibility of the 4-position.[41] Although it is tempting to suggest that **6** with ten sulfate groups is likely to the most active species, detailed work with homogeneous preparations of **6**, either synthetic or isolated from a mixture, will be necessary to decipher the most active structure.

Inhibitor **6** is a potent anticoagulant *in vitro* and *ex vivo*. It selectively inhibits FXIa (Table 1) with an excellent *in vitro* potency of 1.2 μg/mL (~550 nM). In addition to the high potency, this observation is exciting because **6** is the only molecule in the library of focused

heparin-mimetics that inhibits FXIa. The heparin mimetics studied herein have been found to inhibit other enzymes of the coagulation cascade,[28,29,39] and thus were expected to inhibit FXIa. The results highlight significance of the scaffold, probably arising from its ability to place appropriate number of sulfate groups in three-dimensional space complementary to the HBS of FXIa. Importantly, the inhibition of small molecule hydrolysis by **6** remains true also for FXIa's physiological substrate, FIX (Figure 4), which forms the foundation for the anticoagulant potential observed in human plasma and blood.

Although well characterized in terms of its composition, **6** is still a mixture of species. This implies that the true potency of the species of **6** that induces FXIa inhibition is likely to be higher. Assuming that the deca-sulfated species (~45% proportion) is the most active constituent of **6**, a homogeneous deca-sulfated preparation is likely to display an IC_{50} at least 2-fold lower (~275 nM). Inhibitor **6** doubles the clotting time in APTT assay at 96 μg/mL (Figure 6), which is about 17.8-fold lower than that for enoxaparin (5.4 μg/mL).[43] This difference also hold true in studies with human whole blood (Table 4). The plasma and blood clotting tests used here are initial indicators of success suggesting a strong possibility that **6** is likely to demonstrate good *in vivo* anticoagulant potential.

A mechanistic aspect that adds significantly to clinical viability is allostery. Allostery offers a unique opportunity of highly selective recognition, which nature typically exploits to an advantage.[54] Allosteric sites tend to be less conserved in comparison to orthosteric sites in a family of homologous proteins. For example, exosite II of thrombin and factors Xa, IXa and XIa displays considerable sequence variability,[55,56] despite possessing a fairly similar trypsin-like, active site specificity. This greatly facilitates selective targeting of an allosteric site. Michaelis–Menten kinetics revealed a classic allosteric inhibition mechanism (Figure 5). Inhibitor **6**'s allostery arises from binding to the HBS as shown by the nearly ideal competitive binding in the presence of UFH (Figure 6).

Heparin binds to FXIa in two sites. The A3 domain of the heavy chain (Lys252, Lys253, and Lys255) and the catalytic domain (Lys529, Arg530, Arg532, Lys536, and Lys540) possess a HBS each.[24–27] The former appears to major important role in the formation of a ternary complex between a serpin, FXIa and heparin,[24,27] whereas the latter site appears to be more important for allosteric modification (although its role in ternary complexation cannot be completely negated).[26,27] Our study with the catalytic domain of FXIa, which indicates retention of ~100% of inhibitory potency of **6**, suggests that the novel inhibitor does not bind to the A3 domain. Thus, **6** most probably engages a region within or near the HBS present on the catalytic domain of FXIa. Future work using either co-crystallography and/or alanine scanning mutagenesis should help pinpoint the residues involved in interaction with **6**.

The recognition of HBS by **6** is likely to have significant consequences beyond just the allosteric modification of FXIa's active site. It has been recently established that long, anionic chains of endogeneous polyphosphate activate FXI, the zymogen, to FXIa in the presence of thrombin, which potentially propagates the pro-coagulant signal.[57] This polyphosphate activation is likely to proceed through one or both of the HBSs of FXIa. This implies that **6** may also serve to inhibit this procoagulant signal as a competing ligand. Future work will test this possibility.

A unique and important advantage of **6** is that it is readily synthesizable. In this work, **6** was chemically synthesized in one step from the commercially available polyphenolic precursor, pentagalloyl glucoside. This precursor can be easily isolated from natural sources in good yields[58,59] or could be prepared by methanolysis of the naturally abundant tannic acid.[60,61]

This raises a strong possibility that **6** can be obtained on a large scale in relatively inexpensive manner.

Finally, an interesting advantage of allosteric inhibitors is the promise of tunable modulation. Because allostery involves coupling of two distant sites, i.e., the ligand binding site and the biological response site, the nature, extent and mechanism of coupling is significantly dependent on the structure of the ligand. This implies that whereas some allosteric modulators may induce nearly 100% inhibition, others may only be partially efficacious. This concept has allosteric effectors that show varying efficacy (range of 10–70%) thrombin inhibition.[28,62] The efficacy of inhibition of hydrolysis of chromogenic substrate as well as FIX by FXIa is nearly 100%. Yet, it may be possible to design a **6** derivative that displays a variable efficacy, which can be expected to enhance the capability of anticoagulation regulation. In fact, a study of a group of allosteric inhibitors that target thrombin has demonstrated variable inhibition efficacies.[28,63] Sulfated benzofuran monomers and dimers modulate protease function by binding to exosite II, which is the HBS for thrombin. Yet, these allosteric thrombin inhibitors are structurally different from **6** because they contain only one sulfate group in comparison to **6**'s multiple sulfates. Likewise, another group of allosterically active molecules include the polysulfated tetrahydroisoquinolines, which activate antithrombin for the accelerated inhibition of factor Xa.[39] These molecules also occupy the HBS on antithrombin, yet do not directly engage factor Xa or thrombin at all. Thus, despite the structural similarity of **6** with these mono- and poly- sulfated molecules, the interaction of these allosteric molecules with their target proteins are fundamentally different. This bodes well for both the specificity and efficacy of interactions this growing body of sulfated allosteric modifiers.

Overall, **6** is the first allosteric inhibitor of factor XIa that displays good potency in *ex vivo* anticoagulation assays. It possesses many advantages including relatively easy synthesis, allosteric recognition, and high specificity of targeting FXIa. **6** is likely to open up new opportunities for the design of clinically relevant allosteric anticoagulants.

Supplementary Material

Refer to Web version on PubMed Central for supplementary material.

Acknowledgments

This work was supported by grants HL090586 and HL107152 from the National Institutes of Health to URD and by an American Heart Association–Mid-Atlantic Affiliate postdoctoral fellowship to RAAH (grant #12POST10930004).

Abbreviations

APTT	activated partial thromboplastin time
FXI	factor XI
FXIa	factor XIa
FIX	factor IX
FXIa-CD	factor XIa-catalytic domain
GAG	glycosaminoglycan
HBS	heparin binding site
LMWHs	low molecular weight heparins

PT	prothrombin time
SIR	selective ion recording
SCA	sulfated chlorogenic acid
SPGG	sulfated pentagalloylglucoside
SS	sulfated silibinin
TEG	thromboelastography
THIQ	tetrahydroisoquinoline
UFH	unfractionated heparin

References

1. Henry, BL.; Desai, UR. Anticoagulants: Drug discovery and development. In: Rotella, D.; Abraham, DJ., editors. Burger's Medicinal Chemistry. 7th ed.. New York: John Wiley and Sons; 2010. p. 365-408.
2. Bates SM, Weitz JI. The status of new anticoagulants. Br. J. Haematol. 2006; 134:3–19. [PubMed: 16803562]
3. Hirsh J, Anand SS, Halperin JL, Fuster V. Guide to anticoagulant therapy: Heparin: a statement for healthcare professionals from the American Heart Association. Circulation. 2001; 103:2994–3018. [PubMed: 11413093]
4. Ansell J, Hirsh J, Hylek E, Jacobson A, Crowther M, Palareti G. Pharmacology and management of the vitamin K antagonists: American College of Chest Physicians. Evidence-based clinical practice guidelines, 8th ed. Chest. 2008; 133:160S–198S. [PubMed: 18574265]
5. Eikelboom JW, Wallentin L, Connolly SJ, Ezekowitz M, Healey JS, Oldgren J, Yang S, Alings M, Kaatz S, Hohnloser SH, Diener H-C, Franzosi MG, Huber K, Reilly P, Varrone J, Yusuf S. Risk of Bleeding With 2 Doses of Dabigatran Compared With Warfarin in Older and Younger Patients With Atrial Fibrillation. An analysis of the randomized evaluation of long-term anticoagulant therapy (RE-LY) Trial. Circulation. 2011; 123:2363–2372. [PubMed: 21576658]
6. Levine MN. New antithrombotic drugs: Potential for use in oncology. J. Clin. Oncol. 2009; 27:4912–4918. [PubMed: 19738103]
7. Lee AYY. Anticoagulation in the treatment of established venous thromboembolism in patients with cancer. J. Clin. Oncol. 2009; 27:4895–4901. [PubMed: 19738121]
8. Bates SM, Greer IA, Pabinger I, Sofaer S, Hirsh J. American College of Chest Physicians. Venous thromboembolism, thrombophilia, antithrombotic therapy, and pregnancy: American College of Chest Physicians Evidence-Based Clinical Practice Guidelines (8th Ed.). Chest. 2008; 133:844S–886S. [PubMed: 18574280]
9. Schumacher WA, Luettgen JM, Quan ML, Seiffert DA. Inhibition of factor XIa as a new approach to anticoagulation. Arterioscler. Thromb. Vasc. Biol. 2010; 30:388–392. [PubMed: 20139363]
10. Löwenberg EC, Meijers JCM, B. P. Monia BP, Levi M. Coagulation factor XI as a novel target for antithrombotic treatment. J. Thromb. Haemost. 2010; 8:2349–2357. [PubMed: 20727068]
11. Mannucci PM, Bauer KA, Santagostino E, Faioni E, Barzegar S, Coppola R, Rosenberg RD. Activation of the coagulation cascade after infusion of a factor XI concentrate in congenitally deficient patients. Blood. 1994; 84:1314–1319. [PubMed: 8049446]
12. Seligsohn U. FXI deficiency in humans. J. Thromb. Haemost. 2009; 7:84–87. [PubMed: 19630775]
13. Gomez K, Bolton-Maggs P. Factor XI deficiency. Haemophilia. 2008; 14:1183–1189. [PubMed: 18312365]
14. Dusga S, Salomon O. Factor XI deficiency. Semin. Thromb. Hemost. 2009; 35:416–425. [PubMed: 19598070]

15. Salmon O, Steinberg DM, Korean-Morag N, Tanne D, Seligsohn U. Reduced incidence of ischemic stroke in patients with severe factor XI deficiency. Blood. 2008; 111:4113–4117. [PubMed: 18268095]
16. Meijers JCM, Tekelenburg WLH, Bouma BN, Bertina RM, Rosendaal FR. High levels of coagulation factor XI as a risk factor for venous thrombosis. N. Eng. J. Med. 2000; 342:696–701.
17. Berliner JI, Rybicki AC, Kaplan RC, Monrad ES, Freeman R, Billett HH. Elevated levels of factor XI are associated with cardiovascular disease in women. Thromb. Res. 2002; 107:55–60. [PubMed: 12413590]
18. Rosen ED, Gailani D, Castellino FJ. FXI is essential for thrombus formation following $FeCl_3$-induced injury of the carotid artery in the mouse. Thromb. Haemost. 2002; 87:774–776. [PubMed: 12008966]
19. Emsley J, McEwan PA, Gailani D. Structure and function of factor XI. Blood. 2010; 115:2569–2577. [PubMed: 20110423]
20. Seligsohn U. FXI in haemostasis and thrombosis: past, present, and future. Thromb. Haemost. 2007; 98:84–89. [PubMed: 17597996]
21. Baglia FA, Gailani D, López JA, Walsh PN. Identification of a binding site for glycoprotein Ibalpha in the Apple 3 domain of factor XI. J. Biol. Chem. 2004; 279:45470–45476. [PubMed: 15317813]
22. Baglia FA, Shrimpton CN, Emsley J, Kitagawa K, Ruggeri ZM, López JA, Walsh PN. Factor XI interacts with the leucine-rich repeats of glycoprotein Ibalpha on the activated platelet. J Biol Chem. 2004; 279:49323–49329. [PubMed: 15375170]
23. Ho DH, Badellino K, Baglia FA, Walsh PN. A binding site for heparin in the apple 3 domain of factor XI. J. Biol. Chem. 1998; 273:16382–16390. [PubMed: 9632702]
24. Zhao M, Abdel-Razek T, Sun MF, Gailani D. Characterization of a heparin-binding site on the heavy chain of factor XI. J. Biol. Chem. 1998; 273:31153–31159. [PubMed: 9813019]
25. Badellino KO, Walsh PN. Localization of a heparin binding site in the catalytic domain of FXIa. Biochemistry. 2001; 40:7569–7580. [PubMed: 11412111]
26. Sinha D, Badellino KO, Marcinkiewicz M, Walsh PN. Allosteric modification of factor XIa functional activity upon binding to polyanions. Biochemistry. 2004; 43:7593–7600. [PubMed: 15182201]
27. Yang L, Sun MF, Gailani D, Rezaie AR. Characterization of a heparin-binding site on the catalytic domain of factor XIa: mechanism of heparin acceleration of factor XIa inhibition by the serpins antithrombin and C1-inhibitor. Biochemistry. 2009; 48:1517–1524. [PubMed: 19178150]
28. Sidhu PS, Liang A, Mehta AY, Abdel Aziz MH, Zhou Q, Desai UR. Rational design of potent, small, synthetic allosteric inhibitors of thrombin. J. Med. Chem. 2011; 54:5522–5531. [PubMed: 21714536]
29. Abdel Aziz MH, Sidhu PS, Liang A, Kim JY, Mosier PD, Zhou Q, Farrell DH, Desai UR. Designing allosteric regulators of thrombin. Monosulfated benzofuran dimers selectively interact with arg173 of exosite II to induce inhibition. J. Med. Chem. 2012; 55:6888–6897. [PubMed: 22788964]
30. Lin J, Deng H, Jin L, Pandey P, Quinn J, Cantin S, Rynkiewicz MJ, Gorga JC, Bibbins F, Celatka CA, Nagafuji P, Bannister TD, Meyers HV, Babine RE, Hayward NJ, Weaver D, Benjamin H, Stassen F, Abdel-Meguid SS, Strickler JE. Design, synthesis, and biological evaluation of peptidomimetic inhibitors of fXIa as novel anticoagulants. J. Med. Chem. 2006; 49:7781–7791. [PubMed: 17181160]
31. Deng H, Bannister TD, Jin L, Babine RE, Quinn J, Nagafuji P, Celatka CA, Lin J, Lazarova TI, Rynkiewicz MJ, Bibbins F, Pandey P, Gorga J, Meyers HV, Abdel-Meguid SS, Strickler JE. Synthesis, SAR exploration, and X– ray crystal structures of factor XIa inhibitors containing an α-keto- thiazole arginine. Bioorg. Med. Chem. Lett. 2006; 16:3049–3054. [PubMed: 16524727]
32. Lazarova TI, Jin L, Rynkiewicz M, Gorga JC, Bibbins F, Meyers HV, Babine R, Strickler J. Synthesis and in vitro biological evaluation of arylboronic acids as potential inhibitors of factor XIa. Bioorg. Med. Chem. Lett. 2006; 16:5022–5027. [PubMed: 16876411]

33. Schumacher WA, Seiler SE, Steinbacher TE, Stewart AB, Bostwick JS, Hartl KS, Liu EC, Ogletree ML. Antithrombotic and hemostatic effects of a small molecule factor XIa inhibitor in rats. Eur. J. Pharmacol. 2007; 570:167–174. [PubMed: 17597608]
34. Wong PC, Crain EJ, Watson CA, Schumacher WA. A small-molecule factor XIa inhibitor produces antithrombotic efficacy with minimal bleeding time prolongation in rabbits. J. Thromb. Thrombolysis. 2011; 32:129–137. [PubMed: 21614454]
35. Buchanan MS, Carroll AR, Wessling D, Jobling M, Avery VM, Davis RA, Feng Y, Xue Y, Oster L, Fex T, Deinum J, Hooper JN, Quinn RJ. Clavatadine A, a natural product with selective recognition and irreversible inhibition of factor XIa. J. Med. Chem. 2008; 51:3583–3587. [PubMed: 18510371]
36. Hanessian S, Larsson A, Fex T, Knecht W, Blomberg N. Design and synthesis of macrocyclic indoles targeting blood coagulation cascade Factor XIa. Bioorg. Med. Chem. Lett. 2010; 20:6925–6928. [PubMed: 21035339]
37. Fradera X, Kazemier B, Carswell E, Cooke A, Oubrie A, Hamilton W, Dempster M, Krapp S, Nagel S, Jestel A. High-resolution crystal structures of factor XIa coagulation factor in complex with nonbasic high-affinity synthetic inhibitors. Acta Crystallogr Sect F Struct Biol Cryst Commun. 2012; 68(Pt 4):404–408.
38. Sun MF, Zhao M, Gailani D. Identification of amino acids in the factor XI apple 3 domain required for activation of factor IX. J. Biol. Chem. 1999; 274:36373–36378. [PubMed: 10593931]
39. Al-Horani RA, Liang A, Desai UR. Designing nonsaccharide allosteric activators of antithrombin for accelerated inhibition of factor Xa. J. Med. Chem. 2011; 54:6125–6138. [PubMed: 21800826]
40. Al-Horani RA, Desai UR. Electronically rich *N*-substituted tetrahydroisoquinoline-3-carboxylic acid esters: Concise synthesis and conformational studies. Tetrahedron. 2012; 68:2027–2040. [PubMed: 22665943]
41. Raghuraman A, Riaz M, Hindle M, Desai UR. Rapid, high-yielding microwave-assisted per-sulfation of organic scaffolds. Tetrahedron Lett. 2007; 48:6754–6758. [PubMed: 18797498]
42. Henry BL, Thakkar JN, Liang A, Desai UR. Sulfated, low molecular weight lignins inhibit a select group of heparin-binding serine proteases. Biochem. Biophys. Res. Commun. 2012; 417:382–386. [PubMed: 22155248]
43. Henry BL, Thakkar JN, Martin EJ, Brophy DF, Desai UR. Characterization of the plasma and blood anticoagulant potential of structurally and mechanistically novel oligomers of 4-hydroxycinnamic acids. Blood Coagul. Fibrin. 2009; 20:27–34.
44. Correia-da-Silva M, Sousa E, Duarte B, Marques F, Carvalho F, Cunha-Ribeiro LM, Pinto MM. Flavonoids with an oligopolysulfated moiety: a new class of anticoagulant agents. J. Med. Chem. 2011; 54:95–106. [PubMed: 21138266]
45. Correia-da-Silva M, Sousa E, Duarte B, Marques F, Carvalho F, Cunha-Ribeiro LM, Pinto MM. Polysulfated xanthones: multipathway development of a new generation of dual anticoagulant/antiplatelet agents. J. Med. Chem. 2011; 54:5373–5384. [PubMed: 21732671]
46. Correia-da-Silva M, Sousa E, Duarte B, Marques F, Cunha-Ribeiro LM, Pinto MM. Dual anticoagulant/antiplatelet persulfated small molecules. Eur. J. Med. Chem. 2011; 46:2347–2358. [PubMed: 21450376]
47. Gunnarsson GT, Desai UR. Designing small, non-sugar activators of antithrombin using hydropathic interaction analyses. J. Med. Chem. 2002; 45:1233–1243. [PubMed: 11881992]
48. Doneanu CE, Chen W, Gebler JC. Analysis of oligosaccharides derived from heparin by ion-pair reversed-phase chromatography/mass spectrometry. Anal. Chem. 2009; 81:3485–3499. [PubMed: 19344114]
49. Smith SB, Verhamme IM, Sun MF, Bock PE, Gailani D. Characterization of novel forms of coagulation factor XIa: independence of factor XIa subunits in factor IX activation. J. Biol. Chem. 2008; 283:6696–6705. [PubMed: 18192270]
50. Sun Y, Gailani D. Identification of a factor IX binding site on the third apple domain of activated factor XI. J. Biol. Chem. 1996; 271:29023–29028. [PubMed: 8910554]
51. Salooja N, Perry DJ. Thrombelastography. Blood Coagul. Fibrinol. 2001; 12:327–337.
52. Klein SM, Slaughter TF, Vail PT, Ginsberg B, El-Moalem HE, Alexander R, D'Ercole F, Greengrass RA, Perumal TT, Welsby I, Gan TJ. Thromboelastography as a perioperative measure

of anticoagulation resulting from low molecular weight heparin: a comparison with anti-Xa concentrations. Anesth. Analg. 2000; 91:1091–1095. [PubMed: 11049889]

53. Naito K, Fujikawa K. Activation of human blood coagulation factor XI independent of factor XII: factor XI is activated by thrombin and factor XIa in the presence of negatively charged surfaces. J. Biol. Chem. 1991; 266:7353–7358. [PubMed: 2019570]
54. Krishnaswamy S. Exosite-driven substrate specificity and function in coagulation. J. Thromb. Haemost. 2005; 3:54–67. [PubMed: 15634266]
55. Page MJ, Macgillivray RT, Di Cera E. Determinants of specificity in coagulation proteases. J. Thromb. Haemost. 2005; 3:2401–2408. [PubMed: 16241939]
56. Abdel Aziz MH, Mosier PD, Desai UR. Identification of the site of binding of sulfated, low molecular weight lignins on thrombin. Biochem. Biophys. Res. Commun. 2011; 413:348–352. [PubMed: 21893043]
57. Choi SH, Smith SA, Morrissey JH. Polyphosphate is a cofactor for the activation of factor XI by thrombin. Blood. 2011; 118:6963–6970. [PubMed: 21976677]
58. Haslam, E. Plant Polyphenols: Vegetable Tannins Revisited. Cambridge, UK: Cambridge University Pres; 1981. p. 1-13.p. 90-153.
59. Xu S-J, Yang L, Zeng X, Zhang M, Wang Z-T. Characterization of compounds in the Chinese herbal drug Mu-Dan-Pi by liquid chromatography coupled to electrospray ionization mass spectrometry. Rapid Commun. Mass Spectrom. 2006; 20:3275–3288. [PubMed: 17044128]
60. Hagerman, AE.; Zhao, Y.; Johnson, S. Methods for determination of condensed and hydrolysable tannins. In: Shahadi, F., editor. Antinutrients and Phytochemicals in Foods. Washington DC: ACS; 1997. p. 209-222.
61. Chen Y, Hagerman AE. Characterizing soluble non-covalent complexes between bovine serum albumin and β-1,2,3,4,6-penta-O-galloyl-D-glucopyranose by MALDI-TOF mass spectroscopy. J. Agric. Food Chem. 2004; 52:4008–4011. [PubMed: 15186130]
62. Desai BJ, Boothello R, Mehta AY, Scarsdale JN, Wright HT, Desai UR. Interaction of thrombin with sucrose octasulfate. Biochemistry. 2011; 50:6973–6982. [PubMed: 21736375]
63. Verghese J, Liang A, Sidhu PS, Hindle M, Zhou Q, Desai UR. First steps in the direction of synthetic, allosteric, direct inhibitors of thrombin and factor Xa. Bioorg. Med. Chem. Lett. 2009; 19:4126–4129. [PubMed: 19540113]

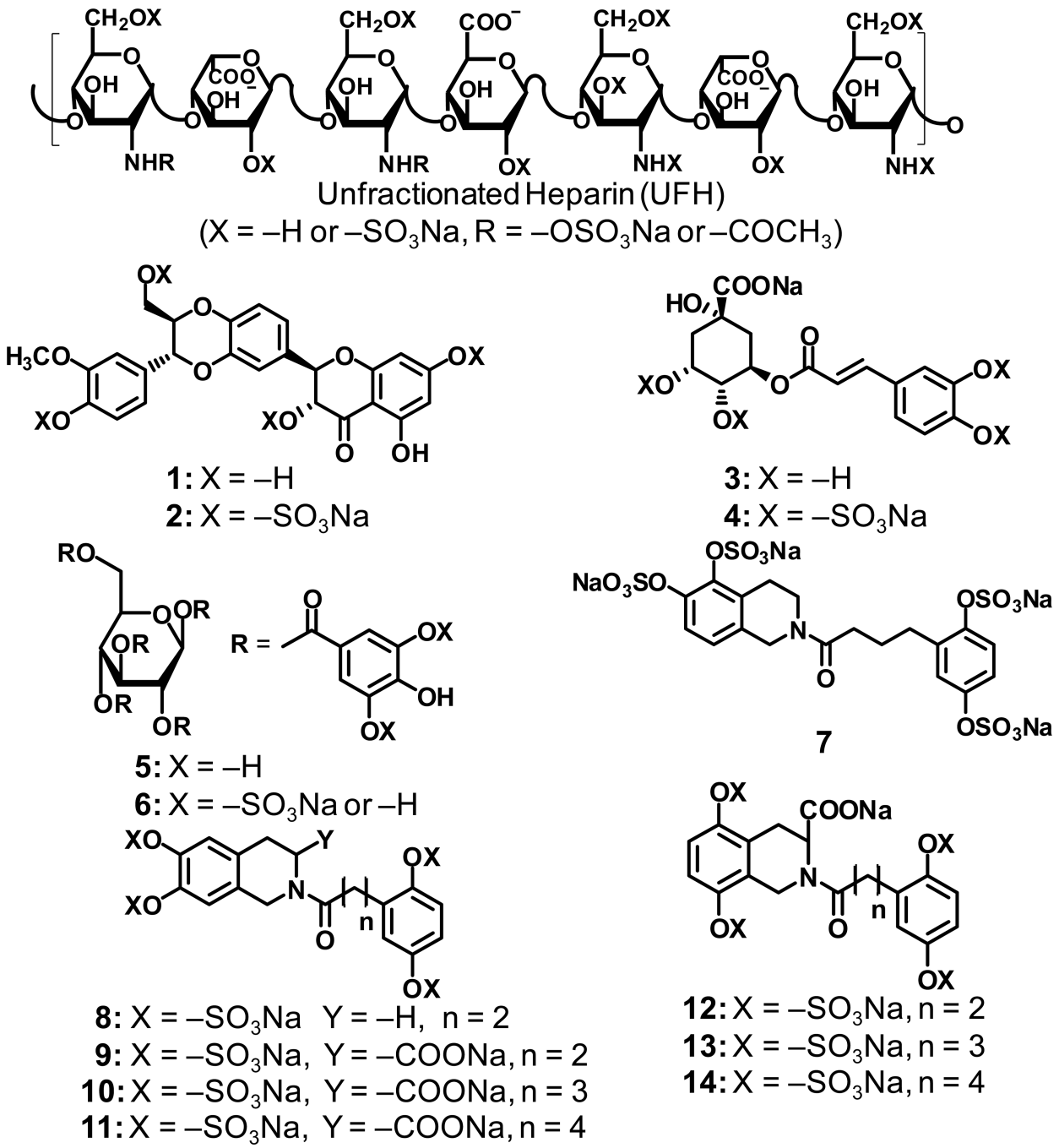

Figure 1. Structures of heparins (A) and the polyphenolic as well as the sulfated molecules were screened against factor XIa (B)

Shown in A are heparins including unfractionated heparin (UFH) (Mwt ~ 15,000 Da) as well as LMWHs (Mwt ~ 4000 Da), both of which are highly heterogeneous and polydisperse mixtures of linear polysulfated polysaccharides. Shown in B are the chemical structures of the diversified library of small molecules which were screened against factor XIa including silibinin (**1**), sulfated silibinin (**2**), chlorogenic acid (**3**), sulfated chlorogenic acid (**4**), pentagalloyl glucopyranoside (**5**), sulfated pentagalloylglucoside (**6**), and tetrahydroisoquinoline–based scaffolds (**7–14**).

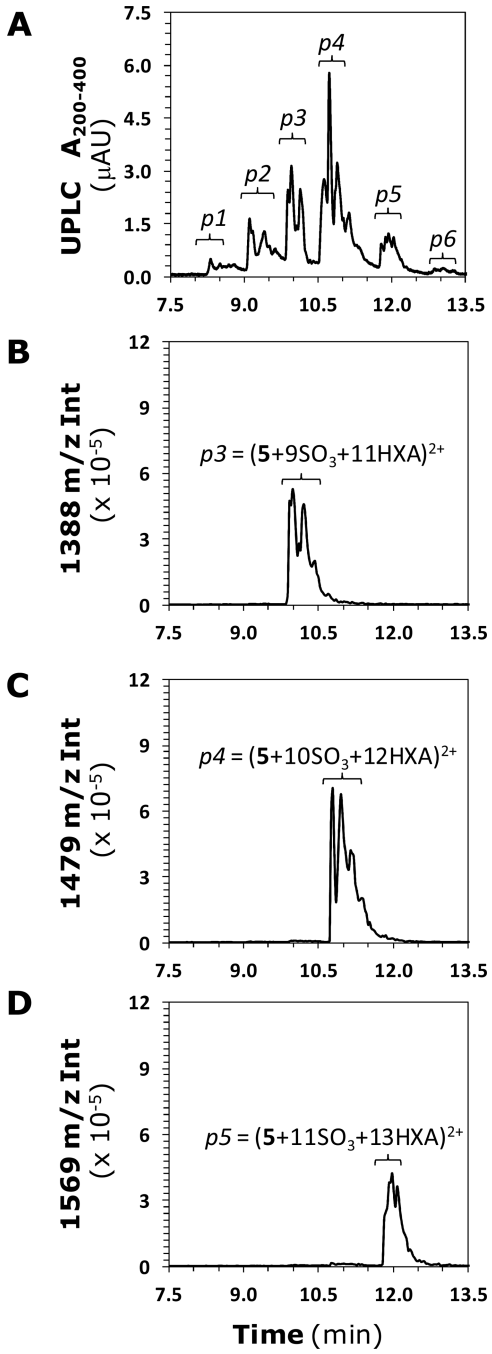

Figure 2. UPLC-MS analysis of the structure of 6

(A) shows UPLC resolution of **6** into six peaks (*p1* to *p6*), which arise from variable sulfation of the PGG scaffold. (B) – (D) show SIR monitoring of **6** at 1388, 1479 and 1569 m/z to identify the peaks corresponding to 9, 10 and 11 sulfated PGG species. Similar SIR profiles were measured for 7, 8 and 12 sulfated species (see Figure S6). See text for detailed interpretation.

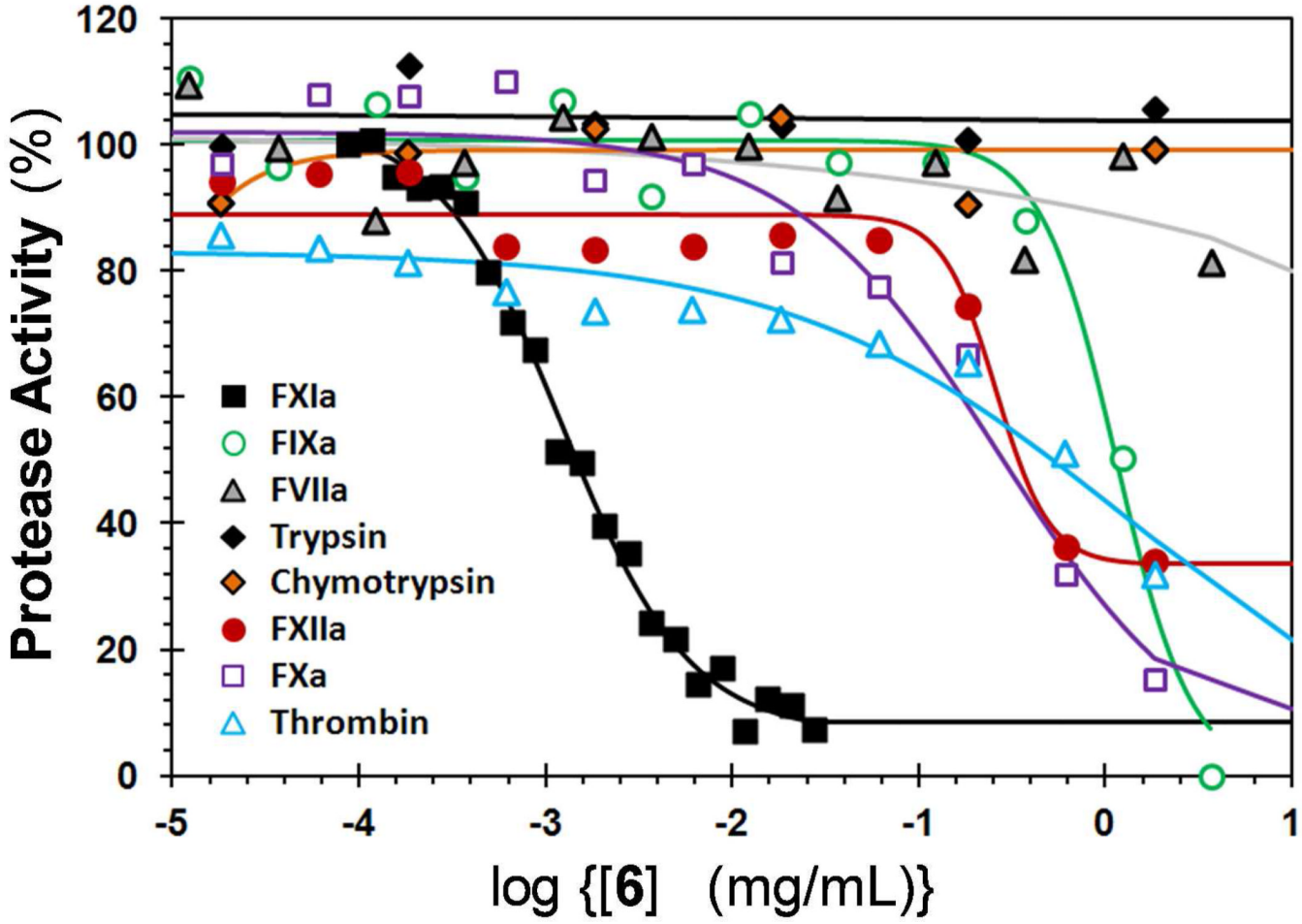

Figure 3. Direct inhibition of coagulation and digestive proteases by 6

The inhibition of factor XIa (■), factor Xa (□), thrombin (△), factor XIIa (●), factor IXa (○), factor VIIa (▲), chymotrypsin (◊), and trypsin (♦) by **6** was studied as described in "Experimental Procedures". Solid lines represent sigmoidal dose–response fits (Eq. 1) to the data to obtain the values of IC_{50}, ΔY, and HS.

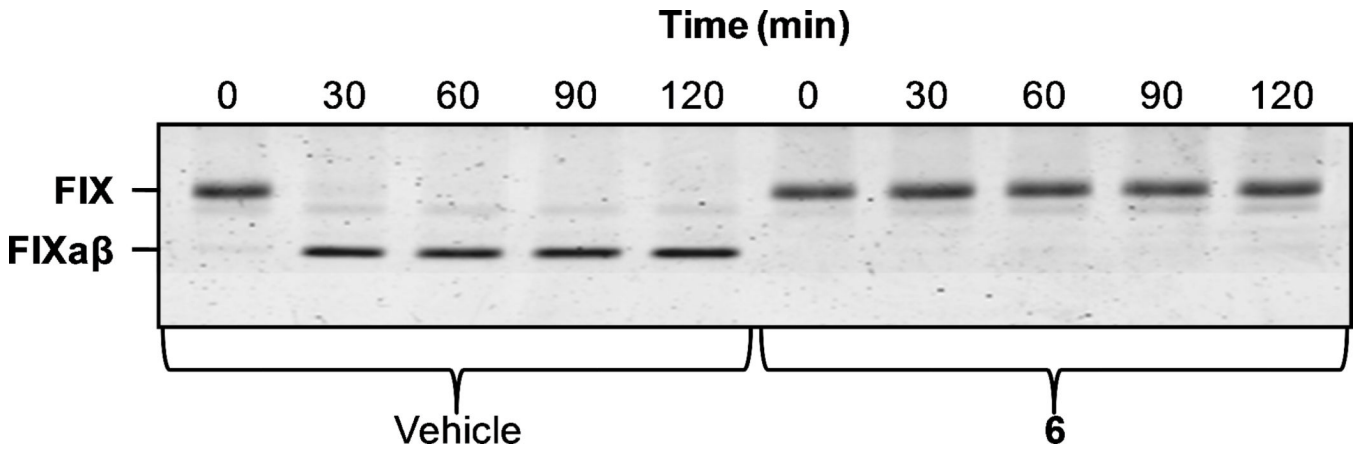

Figure 4. Time course of FIX activation by FXIa in the presence and absence of 6

FIX (500 nM) in the assay buffer was incubated with FXIa (3 nM) and **6** (0 or 3 ±M) and aliquots of the reaction analyzed using standard denaturing polyacrylamide gel electrophoresis followed by Western blotting. See Experimental Procedures for details.

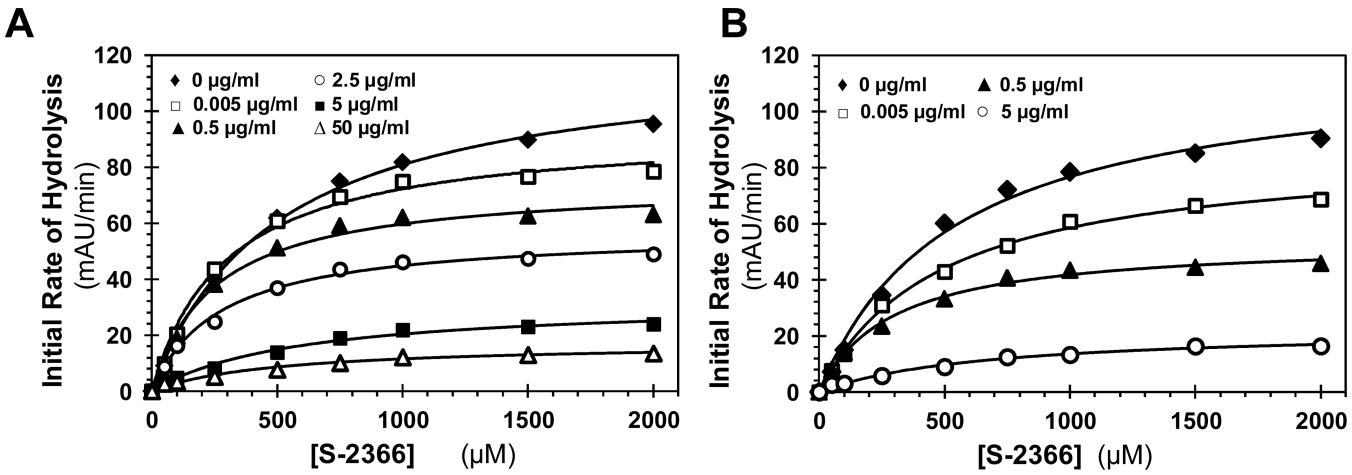

Figure 5. Michaelis–Menten kinetics of S-2366 hydrolysis by factor XIa in the presence of 6

The initial rate of hydrolysis at various substrate concentrations was measured in pH 7.4 buffer as described in "Experimental Procedures" using FXIa wild type (FXIa-WT) (A) and FXIa catalytic domain (FXIa-CD) (B). The concentrations of **6** chosen in the study were in (A) 0 (♦), 0.005 (□), 0.5 (▲), 2.5 (○), 5 (■), 50 μg/mL (△) and in (B) 0 (♦), 0.005 (□), 0.5 (▲), 5 μg/mL (○). Solid lines represent nonlinear regressional fits into the data by the Michaelis–Menten Eq. 2.

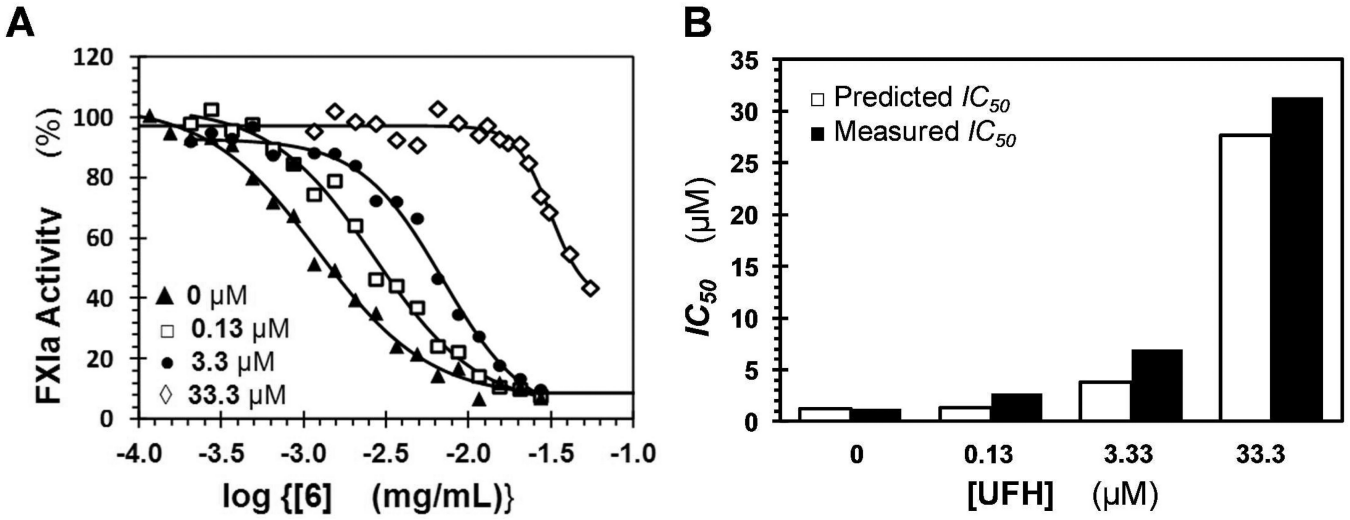

Figure 6. Competitive direct inhibition of factor XIa by 6 in the presence of UFH (A) and comparison of the predicted and experimentally measured IC_{50} (B)

Shown in A is the inhibition of factor XIa by **6** in the presence of UFH which was determined spectrophotometrically at pH 7.4 and 37 °C. Solid lines represent fits by the dose–response Eq. 1 to obtain the $IC_{50,predicted}$, as described in "Experimental Procedures". The concentrations of UFH selected for the study were 0 (▲), 0.13 (□), 3.3 (●), 33.3 μM (◊). Shown in B is comparison of the predicted and experimentally measured IC_{50} FXIa inhibition by **6** in the presence of UFH. Open bars represent the measured values, whereas closed bars are the values predicted using Dixon-Webb Eq.4.

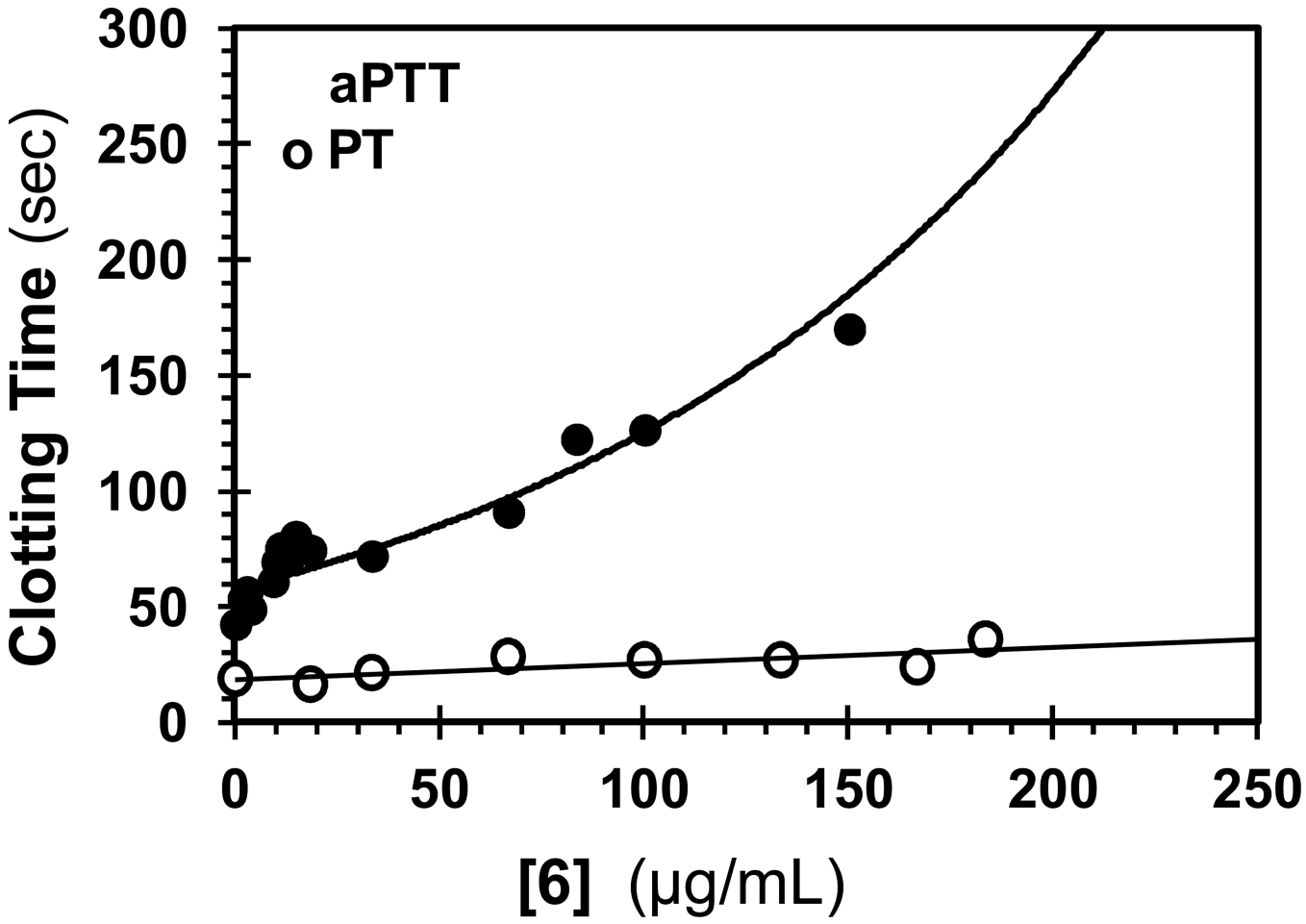

Figure 7. Effect of 6 on the clotting times of PT and APTT in human plasma

Prolongation of clotting time as a function of **6** concentration in either prothrombin time assay (PT) (○) or activated partial thromboplastin time assay (APTT) (●). Solid lines are trend lines from which the concentration necessary to double clotting time was deduced. Clotting assays were performed as described in “Experimental Procedures”.

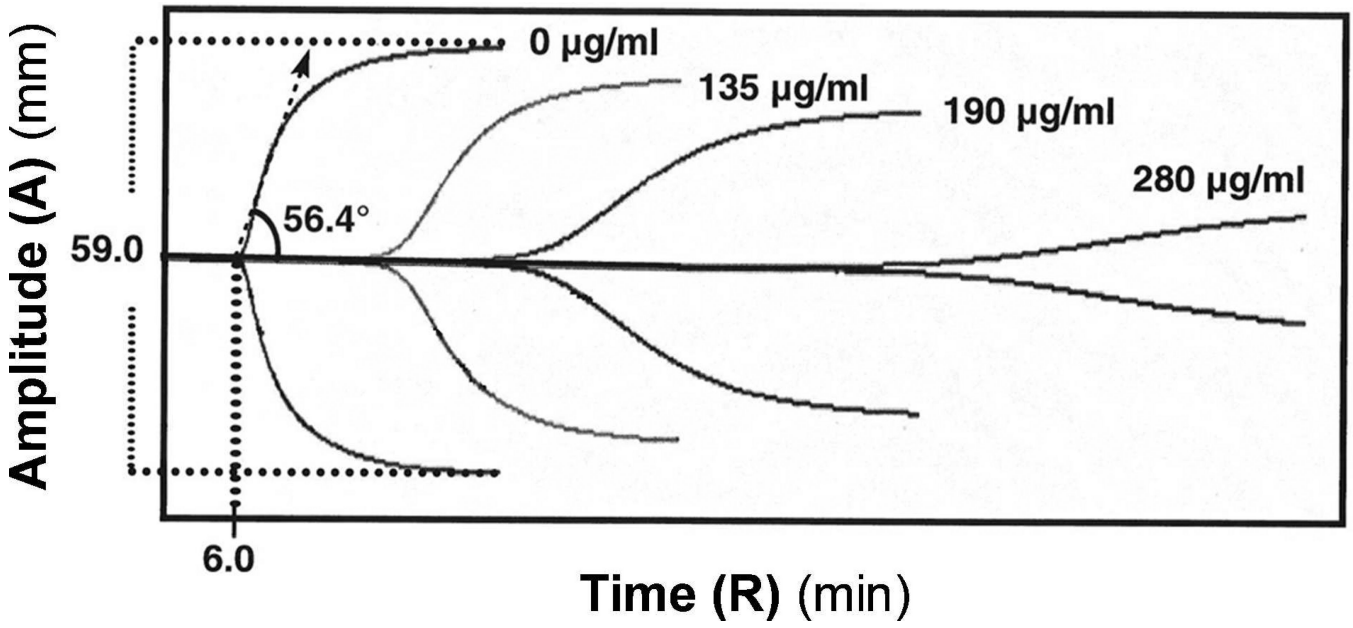

Figure 8. Thromboelastography analysis of clot formation in the presence of 6

Comparison of the effect of **6** and enoxaparin on clot formation in whole blood using thromboelastography analysis. A typical thromboelastogram expected of any anticoagulant is described by R, α, MA, and G parameters. This analysis was performed as described in "Experimental Procedures".

Table 1

Inhibition profile of 6 against coagulation and digestive proteases.[a]

Protease	IC_{50} (μg/mL)	HS	ΔY
Factor XIa	1.2 ± 0.03	1.3 ± 0.1	97.1 ± 3.2
Factor Xa	266 ± 31	0.8 ± 0.2	101.9 ± 3.5
Factor IXa	1141 ± 141[d]	2.2 ± 0.6	100.6 ± 5.8
Factor XIIa	256 ± 28	3.0 ± 1.8	55.7 ± 5.9
Thrombin	1219 ± 202	0.5 ± 0.1	83 ± 10
Factor VIIa	NI[b]	na	na
Trypsin	NI	na[c]	na
Chymotrypsin	NI	na	na

[a]The IC_{50}, HS, and ΔY values were obtained following non-linear regression analysis of direct inhibition of the protease. Inhibition was monitored by spectrophotometric measurement of residual proteases activity (see Experimental Procedures).

[b]No inhibition was observed up to concentrations as high as 1.8 mg/mL for trypsin and chymotrypsin and 3.7 mg/mL for factor VIIa.

[c]Not applicable.

[d]Errors represent ± 1 S.E.

Table 2

Hydrolysis of the chromogenic substrate S-2366 by human factor XIa in the presence of 6. [a]

	[6] (μg/mL)	K_M (mM)	V_{MAX} (mAU/min)
FXIa Wild Type	0	0.50 ± 0.04[b]	120.9 ± 3.1
	0.005	0.30 ± 0.03	93.7 ± 3.2
	0.5	0.25 ± 0.03	74.6 ± 2.6
	2.5	0.30 ± 0.03	56.9 ± 1.5
	5.0	0.60 ± 0.10	32.3 ± 2.1
	50.0	0.50 ± 0.10	17.2 ± 1.2
FXIa Catalytic Domain	0	0.53 ± 0.07	117.3 ± 5.3
	0.005	0.49 ± 0.04	87.0 ± 2.2
	0.5	0.29 ± 0.03	53.9 ± 1.4
	5.0	0.67 ± 0.10	22.6 ± 1.4

[a] K_M and V_{MAX} values of S-2366 substrate hydrolysis by human factor XIa were measured as described under (Experimental Procedures). mAU indicates milliabsorbance units.

[b] Error represents ± 1 S.E.

Table 3

Inhibition of human FXIa by 6 in the presence of UFH at pH 7.4 and 37 °C.[a]

UFH (μM)	IC_{50} (μg/mL)	HS	ΔY	$IC_{50,\ predicted}$ (μg/mL)
0	1.2 ± 0.03[b]	1.3 ± 0.1	97.1 ± 3.2	1.2
0.13	2.7 ± 0.1	1.4 ± 0.2	99.7 ± 5.0	1.3
3.33	7.0 ± 0.3	1.7 ± 0.2	92.7 ± 6.4	3.9
33.3	31 ± 1.0	4.0 ± 0.9	58.2 ± 6.6	27.8

[a]The IC_{50}, HS, and ΔY values were obtained following non-linear regression analysis of direct inhibition of human factor XIa in 50 mM Tris-HCl buffer, pH 7.4, containing 150 mM NaCl, 0.1% PEG8000, and 0.02% Tween80 at 37 °C. Inhibition was monitored by spectrophotometric measurement of residual factor XIa activity (see Experimental Procedures).

[b]Errors represent ± 1 S.E.

Table 4

Human whole blood clotting parameters of 6 by thromboelastography.[a]

	Concentration (μg/mL)	R[b] (min)	α[b] (degs)	MA[b] (mm)	G[b] (kDynes/cm^3)
6	0	6.0[c]	56.4	59	7.2×10^3
	20[d]	6.6	51.4	62	8.2×10^3
	135	22.8	30.6	49.8	5.0×10^3
	190	37.8	9.4	43.5	3.8×10^3
	280	87.1	*ND*[e]	15.1	0.9×10^3
Enoxaparin	0	7.0	59.0	56.5	6.5×10^3
	1.35	8.0	49.0	51.0	5.2×10^3
	2.7	11.5	43.0	47.0	4.4×10^3
	3.4	14.0	41.0	46.0	4.3×10^3
	4.5	17.0	31.5	42.0	3.6×10^3

[a] Thromboelastography parameters were obtained in an automated manner from the TEG Coagulation Analyzer. See Experimental Procedures for a description of the setup.

[b] Parameters obtained from this analysis were **R** (Reaction time which is the time interval between the initiation of coagulation and the appearance of first detectable signal of no less than 2 mm in amplitude), **α** (Angle which is the acute angle between an extension of the R value tracing and the tangent of the maximum slope produced by the TEG tracing), **MA** (Maximum amplitude which is the maximum distance the pin of TEG moves at the end), and **G** (The shear elastic modulus strength which is a calculated parameter (G = 5000 × MA/(100 −MA) and is a measure of clot strength).

[c] The reported values are the mean of two independent experiments which were recorded automatically. SD in each case was less than 10%.

[d] This concentration of **6** is not graphically plotted in figure 6.

[e] Not determined.